Comparison between two analytical models to study the flocculation of mineral clay by polyelectrolytes

Ali, W.; Chassagne, C.

DOI
10.1016/j.csr.2022.104864

Publication date
2022

Document Version
Final published version

Published in
Continental Shelf Research

Continental Shelf Research 250 (2022) 104864

Contents lists available at ScienceDirect

Continental Shelf Research

journal homepage: www.elsevier.com/locate/csr

Research papers

Comparison between two analytical models to study the flocculation of mineral clay by polyelectrolytes

W. Ali *, C. Chassagne

Environmental Fluid Mechanics, Faculty of Civil Engineering and Geosciences, Delft University of Technology, 2600 GA Delft, The Netherlands

ARTICLE INFO

Keywords:
Flocculation
Population balance equation
Logistic growth
Cohesive sediment

ABSTRACT

In the present article two flocculation models, given in Chassagne and Safar (2020) (LG model) and Winterwerp (1998) (S model) are compared. Both models give the time evolution dL/dt where L is the size of a particle undergoing flocculation, and t is the time. The LG model is based on logistic growth theory, whereas the S model is based on the theory originally derived by Smoluchowski. Both models have the advantage of easy implementation in, for instance, large-scale sediment transport numerical models. However, it is found that they do not obey the same kinetics. A series of laboratory experiments is presented where the flocculation of a mineral clay by polyelectrolyte is studied as a function of clay concentration and shear rate. From modelling these experiments, it is found that the LG model reproduces the time dependence of the floc sizes found experimentally, whereas the S model does not. It is shown that the LG model can be used to model the data over the whole range of clay concentration and shear investigated. Based on the study presented in this article, it was found that the average floc growth in time for the clay type and conditions applied in the experiments could be modelled by: $dL/dt = 40 \times 10^{-4} G^{0.75} \times [exp(-2 \times 10^{-4} G^{0.75} t)]/[1 + 20exp(-2 \times 10^{-4} G^{0.75} t)]L$.

1. Introduction

Hydrodynamic models are used in sediment transport models to calculate the advection and diffusion of suspended particles in the water column. For most applications, the sediment typically is decomposed into two or three fractions with associated settling velocities in the 0.1 to 1 mm/s range. For a large number of applications, this decomposition makes it possible to correctly predict the Suspended Particulate Matter (SPM) concentration in space and time (Normant, 2000; Manning and Dyer, 2002; Manning et al., 2006a; Lesser et al., 2004). However, changes in particle properties by flocculation and exposure to shear result in a change in settling velocity over time for a given sediment fraction. These changes are currently poorly accounted for in sediment transport models, resulting in inaccurate predictions in coastal regions where these changes occur. Several studies have thus focused on incorporating flocculation into sediment transport models (Russel et al., 1989; Fettweis, 2008; Many et al., 2016; Manning et al., 2006b). These models, however, are not predictive because they contain adjustable parameters that are fitted to the data and, more importantly, they do not account for specific physical processes such as organic matter-induced flocculation or particle coiling under shear (Chassagne and Safar, 2020). Until now, the models used to describe flocculation have been based on Population Balance Equation (PBE), in which flocculation is represented by the aggregation and break-up of similar colloidal particles, as in salt-induced flocculation. In a recent article (Chassagne, 2021), it was shown that the analytical model based on logistic growth theory (LG model) presented by Chassagne et al. in Chassagne and Safar (2020) could be used to model the flocculation of suspended mineral clay (kaolinite). The suspensions were destabilized by the addition of salt. In particular, it was demonstrated that the LG model (1) reproduces the classical results found for the salt-induced flocculation kinetics at the onset of the experiments and (2) enables to study the flocculation kinetics over the whole duration of the experiment. This last point implies that, by fitting the experimental data over the whole duration of the experiment, it was shown that the measured floc size $L(t)$ time evolution follows the relation $dL/dt = L/t_b - L^2/(L_{eq} t_b)$ predicted by the model, where t_b is a characteristic time and L_{eq} a characteristic size, which are obtained from the fits.

Analytical models like the one presented in Chassagne and Safar (2020), Chassagne (2021) are required in many applications, where estimations of the characteristic timescales of flocculation and the equilibrium floc size of flocs should be done in a fast way. For example, large-scale sediment transport models require flocculation models that can be ran on multiple grid cells at the same time. This prevents models like Population Balance Equations (PBE) models to be used for a system

* Corresponding author.
E-mail address: w.ali@tudelft.nl (W. Ali).

https://doi.org/10.1016/j.csr.2022.104864
Received 28 February 2022; Received in revised form 24 September 2022; Accepted 7 October 2022
Available online 17 October 2022

of more than 3 equations (Shen et al., 2018). The simplest PBE model that can be thought of is a PBE with a single equation. This equation then represents the time evolution of a single class of particles, usually taken to be the D_{50} class (the class that represents the particles of size L whereby 50 percent of all particles have a size smaller than L). Such an equation can obviously not be used for modelling the sediment mass transfer between classes. A minimum of two classes is required for that purpose (Chassagne and Safar, 2020; Shen et al., 2018). A single PBE equation can nonetheless be used under the assumption that all mineral sediment is contained in flocs and that all flocs have the same size $L(t)$ with L varying in time under the influence of environmental conditions (shear stress in particular). Such a single PBE equation is given by Winterwerp in Winterwerp (1998). In-situ studies have demonstrated that floc sizes are indeed dynamic and shear-dependent (Manning and Dyer, 2007; Verney et al., 2011; Van Leussen, 1988; Soulsby et al., 2013). The way to connect the floc size and its Stokes settling velocity – which is the key parameter for large-scale sediment transport models – will not be discussed in the present article but are the topic of numerous publications (Dyer and Manning, 1999; Khelifa and Hill, 2006; Gratiot and Manning, 2004; Manning and Dyer, 2007; Spencer et al., 2010; Spearman et al., 2011; Maggi, 2013; Mehta, 2014).

The aim of the present article is to compare the model introduced by Chassagne and Safar (2020) with the one presented by Winterwerp (1998). In particular, the validity and parametrization of the models will be discussed. A series of laboratory experiments are presented to test the theories, where the flocculation of a mineral clay by polyelectrolyte is studied. This type of flocculation is representative of the flocculation occurring in-situ, whereby mineral clay is found to be bound in different amounts to organic matter, usually in the form of complex mixtures of biopolymers (consisting of polysaccharides, proteins, nucleic acids, lipids and humic substances) (Safar et al., 2019; Deng et al., 2019). The experimental setup allows studying the dependence of flocculation on clay concentration and shear rate, two important parameters that are found in the model presented by Winterwerp.

In Section 2, both models are presented, and their differences are discussed. In Section 3, the material and methods are presented. The results are presented and discussed in Section 4, and the conclusion is given in the last section.

2. Theory

In this section, the two theoretical models that we aim to compare are recalled. In the first subsection, the model derived by Chassagne and Safar (2020) is recalled. This model is based on logistic growth theory and hence will be termed "LG model". In the second subsection, the model presented by Winterwerp (1998) is discussed. This model originates from the work of Smoluchowski and, therefore, will be termed "S model". The differences between the two models are discussed in the third subsection.

2.1. Logistic growth model (LG model)

The logistic growth (LG) model is an empirical model that is found to be very convenient to model the time evolution of colloidal suspensions undergoing flocculation. We refer to Chassagne and Safar (2020), Chassagne (2021) for further details and examples of application. The change of floc size as a function of time is described by the equation:

$$\frac{dL}{dt} = [b(t) - d(t)]\, L \tag{1}$$

whereby the (positive) functions for birth $b(t)$ and decay $d(t)$ are given by:

$$b(t) = \frac{a_b}{t_b}\frac{exp(-t/t_b)}{1 + a_b exp(-t/t_b)} \tag{2}$$

$$d(t) = \frac{a_d}{t_d}\frac{exp(-t/t_d)}{1 + a_d exp(-t/t_d)} \tag{3}$$

The coefficients a_b, t_b, a_d, t_d are to be parameterized. As stated in Chassagne (2020), it is emphasized that the names "birth" and "decay" are solely chosen because they appear with a plus and minus sign in the balance equation Eq. (1). One can easily show that considering only the birth function ($d(t) = 0$) gives as solution a sigmoid function, with a growth that will be limited in time. In other words, at infinite time $dL/dt = 0$ implying that $L(t \to \infty) = L_{eq}$ (even when no decay term is present) where L_{eq} is a value that will depend on parameters such as floc composition, shear rate, salinity, etc. For example, let us consider a flocculation experiment whereby external parameters are fixed (constant shear, given salinity and pH, no addition of organic matter over time), as is the case for flocculation experiments that can be realized in the lab. At $t = 0$ some amount of clay and organic matter are mixed in a jar, at a given shear. By following the evolution of the floc size over time, one will find that the mean floc size indeed follows a sigmoid behaviour, as eventually the flocs will reach an equilibrium size that is strongly dependent on the amount of organic matter present in the jar and the imposed shear rate (Deng et al., 2019; Safar et al., 2019; Shakeel et al., 2020). The growth of flocs is therefore limited by a depletion of free organic matter in the water (unbonded flocculant) and/or because their size is reaching the Kolmogorov microscale, but *not* because there is a steady-state between aggregation and break-up. A steady-state would imply that there would be continuously aggregation and break-up of matter at the surface of a floc. This would be the analogue of the adsorption/desorption of molecules from a surface as is studied in thermodynamics (illustrated for example by a Langmuir isotherm (Langmuir, 1918)). This is a crucial difference between this model and the Smoluchowski model presented in the next section. By introducing a decay term $d(t)$, as we will show in Fig. 9, we will be able to model what happens at longer experimental times, after the initial growth (birth) has occurred. It is indeed usually observed that at these longer timescales, a reduction in size is observed. This reduction in size can be due to two effects (not mutually exclusive): (a) an erosion of the flocs under shear and (b) a coiling of particles under shear. Phenomenon (b) in particular has been observed, both in-situ and in the lab (Safar et al., 2019; Shakeel et al., 2020). This phenomenon leads to flocs of higher density and smaller size. In Fig. 9, a decrease of about 20% in size is such obtained. If only particle sizes are studied, this significant reduction in floc size could be mistaken for the breaking of flocs over time, but microscopic observation of the flocs over time have confirmed this densification (Shakeel et al., 2020). The analytical solution of Eq. (1) is given by:

$$L(t) = L_{eq}\frac{1 + a_d exp(-t/t_d)}{1 + a_b exp(-t/t_b)} \tag{4}$$

where $L_{eq} = L(t \to \infty)$. The size L_{eq} can be seen as the size that the floc would reach provided that all parameters (concentration, shear stress, salinity...) remain constant over time. Note that the change in number of flocs per unit volume as function of time can be modelled with an equation similar to Eq. (4) where a_d, a_b, t_d, t_b are (different) adjustable parameters (Chassagne and Safar, 2020):

$$n(t) = n_\infty\frac{1 + a_d exp(-t/t_d)}{1 + a_b exp(-t/t_b)} \tag{5}$$

where $n_\infty = n(t \to \infty)$. At times such that $t \to 0$ implying that $t \ll t_b, t_d$ Eq. (4) reduces to:

$$L(t \to 0) = L(t = 0) + \left(\frac{dL}{dt}\right)_{t=0} t \tag{6}$$

where the flocculation rate $\left(\frac{dL}{dt}\right)_{t=0}$ and size at origin $L(t = 0)$ are defined by:

$$\left(\frac{dL}{dt}\right)_{t=0} = (k_b - k_d)\, L(t = 0) \tag{7}$$

$$L(t = 0) = \frac{1 + a_d}{1 + a_b} L_{eq} \tag{8}$$

When $L(t=0) < L_{eq}$ it follows that $a_d < a_b$ and vice versa. The growth and decay rates k_b and k_d as given by:

$$k_b = \frac{a_b/t_b}{(1+a_b)} \tag{9}$$

$$k_d = \frac{a_d/t_d}{(1+a_d)} \tag{10}$$

2.2. Smoluchowski model (S model)

Smoluchowski introduced in 1917 the Population Balance Equations (PBE) which give the time evolution of classes of colloidal particles (flocs), a class i being defined as a collection of particles with concentration n_i, all particles in class i having the same size (diameter) L_i. The concentrations n_i can either be given in number, mass or volume of particles per unit of volume (Chassagne, 2020; Elimelech et al., 1995). Many studies have since then proposed aggregation and break-up parameters to be implemented in PBE's (Elimelech et al., 1995; Russel et al., 1989; Barthelmes et al., 2003; Spicer and Pratsinis, 1996; Kusters, 1991; Flesch et al., 1999).

The simplest PBE model that can be proposed is the one equation PBE which we call the "S model". This equation represents the time evolution of a single class defined by a concentration $n(t)$ and an average particle size $L(t)$. Unlike the LG model, the S model contains parameters related to the aggregation and break-up properties of the particles. These parameters are, in particular, functions of concentration and shear.

In order to set-up an equation for the average particle size $L(t)$ as function of time first the link between $L(t)$ and the total number of particles (flocs) per unit of volume $n(t)$ and the number of primary particles within a floc $N(t)$ should be made. This is done in the first subsection, where we follow the approach used by Winterwerp (Winterwerp, 1998), who assumes that flocs are fractal objects. The Smoluchowski equation, which expresses the time evolution of $n(t)$, will then be converted into an equation for the time evolution of $L(t)$. This is done in the second subsection.

2.2.1. Link between L, n and N

We define $n(t) = \sum N_i(t)$ as the total number of particles (flocs) per unit of volume at time t and $N_i(t)$ as the number of primary particles inside a floc of size $L_i(t)$. Primary particles are defined as the smallest size of particles in the system. These particles have a size L_p and it is assumed that primary particles cannot break. By aggregation of primary particles, flocs can be formed. By break-up of flocs, smaller flocs are produced and the particles having the smallest size that can be produced are primary particles.

If one defines $n_0 = n(t=0)$ to be the number of unflocculated primary mineral sediment particles per unit of volume in a closed volume (as for example, in a jar test experiment), it follows that n_0 is a constant as function of time, whereas the size L_i of particles in suspension will be time-dependent as flocs are growing (or breaking). The total number of primary particles per unit of volume is given by:

$$n_0 = \sum_i N_i n_i \tag{11}$$

Note that $N_1 = 1$ with $L_1 = L_p$ and that at $t = 0$, $n_0 = n_1$. If it is assumed that, at any moment in time, a suspension is well represented by a characteristic size and concentration, one may write:

$$\begin{aligned} n_0 &= n(t)N(t) \\ 0 &= \frac{dn}{dt}N + n\frac{dN}{dt} \end{aligned} \tag{12}$$

We have here made the assumption that only one class i is present at each time and hence $n(t) = n_{i(t)}(t)$, where the number $i(t)$ of the class is changing at each time step. From Eq. (12), it follows that, when i increases $L = L_i$ and $N = N_i$ increase and hence $n = n_i$ decreases. One may deduce that the rate of decrease of n is given by:

$$\frac{dn}{dt} = \frac{-1}{n_0}\frac{dN}{dt}n^2 \tag{13}$$

The relation between number of primary particles in a floc and floc size is given by Kranenburg (1994):

$$N(t) = \left(\frac{L(t)}{L_p}\right)^D \tag{14}$$

where D is usually termed "fractal dimension", in reference to the study of the flocculation of monodisperse primary particles, where the concept of self-similarity can be used. Experiments have been conducted to assess the fractal dimension for diffusion-limited, and reaction-limited aggregates (Russel et al., 1989), where the initial growth of flocs is also investigated. Combining Eqs. (12) and (14) gives:

$$\frac{1}{n}\frac{dn}{dt} = -\frac{1}{N}\frac{dN}{dt} = -\frac{D}{L}\frac{dL}{dt} \tag{15}$$

The volume fraction of primary particles (pp) inside a floc can be evaluated using:

$$\phi_{pp\ in\ floc} = \frac{V_{pp\ in\ a\ floc}}{V} = \frac{N \times V_p}{V} = N\left(\frac{L_p}{L}\right)^3 = \left(\frac{L_p}{L}\right)^{3-D} \tag{16}$$

where $V_{pp\ in\ a\ floc}$ is the volume occupied by primary particles inside a floc, V_p is the volume of a primary particle and $V \simeq L^3$ the volume of a floc. We have here implicitly assumed that Class 1 and Class $i(t)$ particles have the same shape. If this is not the case, a corresponding multiplying constant should be inserted in the bracket term. The volume fraction $\phi_{pp\ in\ floc}$ is a measurable quantity, as it can be linked to the floc density ρ_{floc} (to be estimated from the settling velocity of floc, applying Stokes' law) by realizing that:

$$\phi_{pp\ in\ floc} = \frac{\rho_{floc} - \rho_w}{\rho_s - \rho_w} \tag{17}$$

where ρ_w is the absolute density of the suspending medium (water), assuming that all the primary particles are contained in flocs (no primary particles are left unflocculated), one gets:

$$\phi_{pp\ in\ floc} = \frac{n \times V_{pp\ in\ floc}}{n \times V} = \frac{\phi_s}{nV} \tag{18}$$

where $\phi_s = c/\rho_s = n_0 L_p^3$ is the volume fraction of primary particles in suspension, ρ_s is the absolute density of a primary particle and c the mass concentration ($\mathrm{kg/m^3}$) of primary particles in suspension. Combining Eqs. (16) and (18):

$$\frac{dn}{dt} = -D\frac{c}{\rho_s}\frac{L^{-D}}{L_p^{3-D}}\frac{1}{D}\frac{dL}{dt} \tag{19}$$

By comparing with Eq. (15), one finds the relation between number n of particles in suspension, number N of primary particles in a floc, size L of flocs and concentration of primary particles:

$$n = \frac{c}{\rho_s}\frac{L^{-D}}{L_p^{3-D}} = \frac{c}{NL_p^3\rho_s} \tag{20}$$

2.2.2. Time evolution of the mean floc size L

One obtains, from the analysis originally performed by Smoluchowski (Elimelech et al., 1995; Chassagne, 2020; Russel et al., 1989) that the rate of change of the number of particles in suspension is given by:

$$\frac{dn}{dt} = -\frac{1}{2}\alpha\beta n^2 \tag{21}$$

In Eq. (21) the collision efficiency α and collision frequency β are class-independent, which is the underlying assumption made by Smoluchowski. The factor $1/2$ that appears in Eq. (21) originates from the fact that each binary collision leads to the loss of two particles of class $i(t)$ and the creation of one particle of class $i(t+dt)$. The dependence of the flocculation rate on shear is usually expressed through the dependence

of the collision frequency on shear in the case of orthokinetic flocculation. This dependence can be expressed as (Elimelech et al., 1995; Chassagne, 2020):

$$\beta \simeq 4GL^3 \tag{22}$$

in the case that all particles at time t have the same size $L(t)$ as is assumed in this subsection. The collision efficiency α is usually assumed to be independent of shear.

Combining Eqs. (15), (20) and (21) one gets:

$$\frac{dL}{dt} = \frac{2\alpha G}{D}\frac{c}{\rho_s}\frac{L^{4-D}}{L_p^{3-D}} = k_A c G L^{4-D} \tag{23}$$

which corresponds to Eqs. (14), (15) proposed by Winterwerp (1998) but for a different prefactor as is detailed in Appendix. One notes that k_A is a function of the fractal dimension D and primary particle size L_p and that k_A does a-priori not depend on shear or concentration. This formulation for dL/dt, based on the Smoluchowski approximation, does not account for a limit in growth which implies that L is bound to increase in time to reach unrealistic values. For this reason, breakup functions are introduced to limit the growth (Chassagne, 2020). The approach used by Winterwerp is to use a function that is scaling as:

$$\frac{dn}{dt} = -s \times n \tag{24}$$

where s is the break-up rate. Winterwerp expresses the change in particle concentration due to breakage as:

$$\frac{dn}{dt} = e_b \times s \times n \tag{25}$$

where e_b is an "efficiency parameter" which is superfluous as it can implicitly be included in s. Note the minus sign difference between Eqs. (24) and (25). The break-up function in the PBE equation appears both with a + and - sign: written like in Eq. (24) it expresses the reduction in the number of flocs when flocs are leaving the size class by breaking, whereas written like Eq. (25) it expresses the increase in the number of flocs in a size class due to the breakage of flocs of larger size. In order to limit the size of flocs, Eq. (25) should be used, as increasing n implies decreasing L. A simple expression for s is of the form (Spicer and Pratsinis, 1996; Barthelmes et al., 2003):

$$s = s_b \left(\frac{\eta G}{\tau^*}\right)^q L^p \tag{26}$$

where s_b, q and p are parameters to be fitted, η is the viscosity of the suspension, and τ^* is characteristic shear stress which is a measure for the aggregate strength: the larger τ^*, the less the particles are susceptible for breakage. An expression for τ^* is given by Eq. (64). The product ηG is the shear stress in shear flows: the higher the stress, the more flocs are susceptible to break.

Combining Eqs. (15), (20) and (26) one gets:

$$\frac{dL}{dt} = \frac{-s_b}{D}\left(\frac{\eta G}{\tau^*}\right)^q L^{p+1} = -k_B G^q L^{p+1} \tag{27}$$

which is to be compared with eq. (23) of Winterwerp (1998):

$$\frac{dL}{dt} = -k_B G^q (L - L_p)^{(p+1)-(2q-1)} L^{(2q-1)} \tag{28}$$

The derivation of this expression is given in Appendix. One notes that k_B is a function of the fractal dimension D, primary particle size L_p, viscosity η and rupture force F and that k_B is a-priori not dependent on concentration c or shear stress G. Combining Eqs. (23) and (27) gives:

$$\frac{dL}{dt} = k_A c G L^{4-D} - k_B G^q L^{p+1} \tag{29}$$

The full flocculation model proposed by Winterwerp is given as eq. (26) in Winterwerp (1998), where aggregation and breakage terms are combined. Winterwerp uses $p = 2$, $q = 1.5$ and $D = 2$ which leads to:

$$\frac{dL}{dt} = \left[k_A c G - k_B G^{3/2}(L - L_p)\right] L^2 \tag{30}$$

The reason that Winterwerp introduces the term $(L - L_p)$ in Eq. (28) as opposed to L in Eq. (27) arises from the fact that at steady-state (when $dL/dt = 0$), Eq. (30) then enables to write, see eq. (27) in Winterwerp (1998):

$$L_{eq} = L_p + \frac{k_A}{k_B} c G^{-1/2} \tag{31}$$

The underlying assumption is that particles can never become smaller than the primary particles, which are assumed insensitive to shear. Eq. (29) leads to:

$$L_{eq}^{D+p-3} = \frac{c k_A}{k_B} G^{1-q} \tag{32}$$

Eq. (31) implies that Eq. (30) can be written as a function of L_{eq} which gives:

$$\frac{dL}{dt} = k_B G^{3/2}\left(L_{eq} - L\right) L^2 \tag{33}$$

One can note that this equation, for a constant shear, can only describe the growth of the mean particle size with time for $L \leq L_{eq}$ since the term at the right-hand side of the equal sign is then positive or zero.

2.3. Comparison between models

In the S model, both aggregation and breakup terms are required to limit floc growth. When no breakup term is present, the aggregation term will ensure that growth is unconstrained, leading to non-physical results. In the LG model, both birth and decay functions are constrained: even with only a birth function $b(t)$ a finite equilibrium size L_{eq} is reached. In flocculation experiments, a suspension of aggregating particles can reach an equilibrium size for different reasons. Growth can be prevented for particles above a characteristic size (related in general to the Kolmogorov microscale) because high shear stresses make it impossible for particles to aggregate. But growth can also be limited because of a depletion of flocculating agent. This happens when polymeric flocculant is underdosed (Shakeel et al., 2020) even when the shear stresses would allow further growth. In the S model, this would imply that k_B is dependent on flocculant dosage.

For the LG model, the evolution of the mean particle size for aggregating particles is described by setting $a_d = 0$ (i.e. $k_d = 0$) in Eq. (4) which then reduces to

$$L(t) = L_{eq}\frac{1}{1 + a_b \exp\left(-t/t_b\right)} \tag{34}$$

with

$$\frac{dL}{dt} = \left(\frac{1}{L} - \frac{1}{L_{eq}}\right)\frac{1}{t_b}L^2 \tag{35}$$

As was discussed earlier in this article, considering only the birth function $b(t)$ only means that the particle size L is an *increasing* function in time. Introducing a decay function $d(t)$ would imply that the size L goes through a maximum as function of time. Clearly, from considering Eq. (33) the S model does not allow for L to go through a maximum (provided that k_B and G are constant — which we assume here), therefore, in order to compare both models, Eq. (35) is to be compared with Eq. (33). Both equations describe the growth of the mean particle size over time but not with the same kinetics. It was shown in Chassagne (2021) that Eq. (35) can be used to follow the time evolution of particles sizes for kaolinite suspensions destabilized by the addition of salt. This meant that by plotting the experimental data according to the function $(dL/dt)/L$ a linear dependence on L was found. The LG model indeed predicts a linear dependence, as is found by rewriting Eq. (35) as:

$$\frac{1}{L}\frac{dL}{dt} = \frac{1}{t_b}\left(1 - \frac{L}{L_{eq}}\right) \tag{36}$$

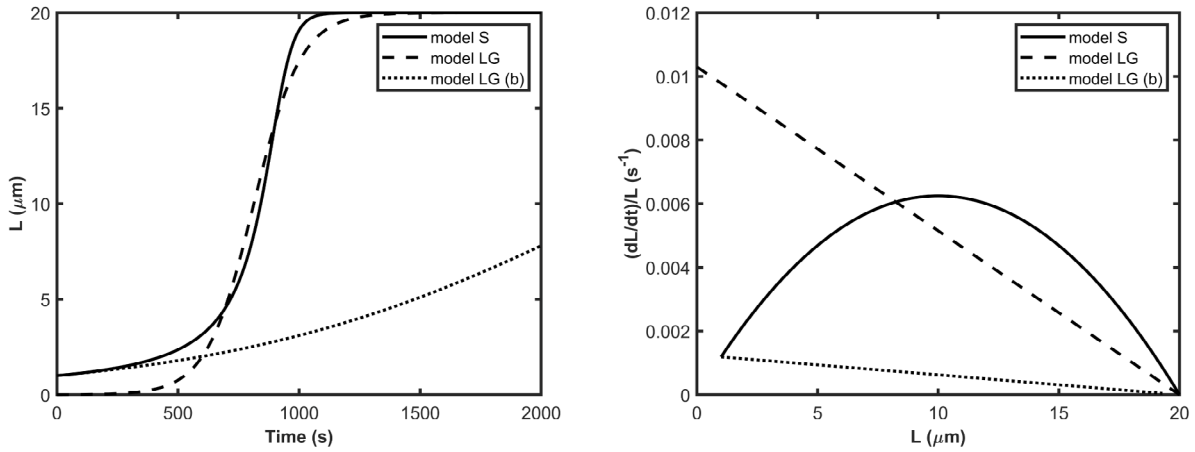

Fig. 1. Comparison between the LG model and S model (left) and their flocculation kinetics (right). The S model is plotted according to Eq. (33) and the LG model according to Eq. (35). The characteristic growth time, equilibrium floc size and primary particle size are taken to be $t_b = 800$ s, $L_{eq} = 20$ μm and $L_p = 1$ μm. The curves corresponding to model LG (b) are obtained using the equivalence of the two models at short timescales, i.e. Eq. (38). The curve obtained for the S model was fitted using Eq. (34), which leads to the dashed curve (LG model). For this fit, it was necessary to use $t_b = 97$ s and $L_p = 0.0046$ μm.

The S model on the other hand predicts a quadratic dependence, see Eq. (31):

$$\frac{1}{L}\frac{dL}{dt} = k_B G^{3/2}\left(L_{eq} - L\right) L \tag{37}$$

The difference between the two models is illustrated in Fig. 1 (left). The S model was plotted according to Eq. (33) and the LG model according to Eq. (35). The characteristic growth time, equilibrium floc size and primary particle size were taken to be $t_b = 800$ s, $L_{eq} = 20$ μm and $L_p = 1$ μm. We made use of the equivalence between the two models at short timescales to evaluate the other required parameters, which can be found using the following equalities:

$$k_B G^{3/2} = \frac{k_A c G L_p}{\left(L_{eq} - L_p\right) L_p} = \frac{k_b}{\left(L_{eq} - L_p\right) L_p} = \frac{1}{t_b}\frac{1}{L_p L_{eq}} \tag{38}$$

Using these parameters, the LG model would give the dotted curve (LG model (b)). At small timescales, the S model and the LG model (b) overlap as expected. The curve obtained for the S model was then fitted using Eq. (34), which leads to the dashed curve (LG model). For this fit, it was necessary to use $t_b = 97$ s and $L_p = 0.0046$ μm. The difference between the flocculation kinetics of the two models is better illustrated in Fig. 1(right), where $(dL/dt)/L$ is plotted for each model: the LG model predicts a linear dependence on L whereas the S model does not. For salt-induced flocculation, it was shown that the linear dependence of $(dL/dt)/L$ on L is also found for the experimental data (Chassagne, 2021). It remains to be studied whether a similar dependence can be observed for polyelectrolyte-induced flocculation.

2.3.1. Short timescales

At short times, one gets for the LG model, from Eq. (7), and assuming that $L(t=0) \simeq L_p$:

$$\left(\frac{1}{L}\frac{dL}{dt}\right)_{t\to 0} = k_b(1 - k_b t) \tag{39}$$

$$\left(\frac{dL}{dt}\right)_{t=0} = k_b L(t=0) = \frac{a_b/t_b}{\left(1+a_b\right)^2} L_{eq} \tag{40}$$

with,

$$L(t=0) \simeq L_p = \frac{1}{1+a_b} L_{eq} \tag{41}$$

For the S model, Eqs. (30) and (33) lead to

$$\left(\frac{dL}{dt}\right)_{t=0} = k_A c G L_p^2 = k_B G^{3/2}\left(L_{eq} - L_p\right) L_p^2 \tag{42}$$

It is therefore easy to make the equivalence between the two models:

$$k_b = \frac{a_b}{t_b}\frac{1}{1+a_b} = \frac{1}{t_b}\frac{L_p}{L_{eq}}\left(1 - \frac{L_p}{L_{eq}}\right) = k_A c G L_p \tag{43}$$

This relation suggests that the birth rate at the onset of aggregation should be linearly dependent on shear and the concentration of primary particles. Note that as it is found in most cases that $a_b \gg 1$, we also get:

$$k_b \simeq \frac{1}{t_b} \tag{44}$$

3. Material and experimental setup

3.1. Clay

The clay used in all the experiments, referred to as K-10.000, was bought from the VE-KA company (Werkendam, The Netherlands). The original lump of clay's water content was 37.5 %, and the sand content was 21 %. The clay was dispersed in tap water and the resulting suspension had a conductivity of less than 453.1 μs cm^{-1} (Shakeel et al., 2020). A Malvern Mastersizer 2000, a technique based on static light scattering (SLS) (Ibanez Sanz, 2018), was used to determine the Particle Size Distribution (PSD) of the clay. This clay was chosen because of its fairly monodispersity: the original clay suspension was found to have a mean diameter (D_{50}) of 5.6 μm. The clay is composed in majority of non-swelling components (Shakeel et al., 2020).

3.2. Flocculant

In order to study the effect of clay concentration on the flocculation rate, different clay concentrations were used in combination with the anionic flocculant Zetag 4110 (BASF). The flocculant to clay concentration ratio was kept the same for all experiments, and equal to 2.5 mg /g, which is close to the optimal concentration for flocculation (Shakeel et al., 2020). Zetag 4110 has a medium anionic charge with high molecular weight.

3.3. Particle/flocs size distribution

The flocculation experiments were performed in a JLT6 jar test set-up provided by VELP Scientifica, Italy. The size of the jar was 95 mm in diameter and 110 mm in height. A single rectangular paddle was used to stir the suspension. The paddle was 25 mm in height and 75 mm in diameter and was positioned in the suspension 10 mm above the bottom of the jar. With the help of a peristaltic pump, the suspension was pumped through the Malvern Mastersizer 2000 from the mixing jar to the Mastersizer and then back to the mixing jar (Fig. 2). This configuration allowed us to control the pump speed and the mixing

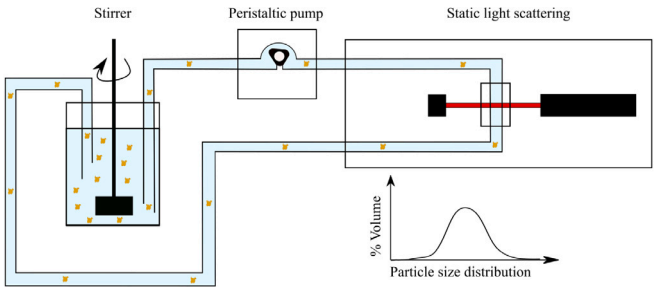

Fig. 2. Schematic of the experimental setup used for measuring particle size.

jar paddle independently. The inner diameter of the connecting tubes was 5 mm, and the overall length was as short as possible, i.e. 2400 mm from the jar and back to the jar. The average shear rate in the jar was chosen to be the lowest possible shear rate that prevents particles settling, i.e. 75 rpm, corresponding to less than $50\,s^{-1}$ (Bouyer et al., 2005). The discharge rate Q of the pump is connected to the shear rate G in the tubes by:

$$G = \frac{4Q}{\pi r^3}$$

where r = 2.5 mm is the radius of the connecting tube. Preliminary experiments, done by varying the shear stress in the jar and connecting tubes, confirmed that the change in the size of flocs mainly occurred in the connecting tubes. The lowest possible discharge rate of the pump was $1.37\,mL\,s^{-1}$ ($112\,s^{-1}$). The shear rate was adjusted by changing the pump discharge rate. With this set-up, every 30 s, it was possible to record a full PSD. All experiments were carried out at room temperature.

4. Results and discussion

4.1. Flocculation kinetics

In this subsection, the particle size time evolution is given in Fig. 3 (top panel) for three examples. It can be noted that the $c = 0.2\,g\,L^{-1}$ sample displays multimodal particle size distributions, which makes the analysis in terms of mean particle size (D_{50}) difficult. The data for $0.2\,g\,L^{-1}$ was therefore not further considered in this study. The data was subsequently plotted in a different way to test Eqs. (36), (37) and (39). The result is given in Fig. 4, where L symbolizes $D_{50}(t)$. From the trends, it appears that at the onset of flocculation, the data plotted as $(dL/dt)/L$ indeed follows the linear dependence predicted by Eqs. (36) and (39). This implies that the flocculation kinetics follow the dependence predicted by the LG model, which is in line with the trends found for salt-induced flocculation discussed in Chassagne (2021). This dependence cannot be obtained from the S model. If the S model is reduced to its aggregation part (the term involving k_A in Eq. (30)), it would still not reproduce the observed behaviour as the S model predicts an increase of $(dL/dt)/L$ as a function of L, not a decrease as observed. A constant increase in $(dL/dt)/L$ would imply an exponential growth of L with time. Such exponential growth is not observed experimentally.

In order to study the flocculation dynamics as function of time, the data for $c = 1.2\,g\,L^{-1}$ was fitted for different time intervals Δt. These time intervals are defined as $\Delta t = [0\ t_{fit}]$, where t_{fit} can be varied. An illustration is given in Fig. 5. The LG model is used for fitting. The model results for several time intervals Δt are shown in Fig. 5 (right). The relation between L_{eq} and $k_b \simeq 1/t_b$ is represented in Fig. 5 (left). It is found that both L_{eq} and t_b are increasing linear functions of Δt until $\Delta t = 1000$ s, and

$$L_{eq}\,(\mu m) = 1.54 t_b^{1.15}$$

$$t_b = 0.2\Delta t \tag{45}$$

It was also found that the parameter a_b could be set constant, as it barely varied with the time interval durations. It was set to its average value of 16.6.

The reason that L_{eq} and k_b are functions of the time interval Δt is due to the change in flocculation kinetics. At the start of flocculation, when clay and polyelectrolyte are mixed, the clay particles will extremely rapidly bind to the bare polyelectrolyte strands. For the smallest time intervals giving meaningful results ($\Delta t = 90$ s), it is found that $L(0) = 7.8$ μm which is in agreement with the clay primary particles size. For longer fitting time intervals, $L(0)$ becomes a function of Δt for $t \lesssim 1500$ s as $L(0)$ and L_{eq} are linked by Eq. (41). It is then found that $L(0)$ is increasing linearly with Δt. During the period $t \lesssim 1500$ s two types of flocculation occur: (a) the remaining mineral clay particles in suspension (if any) are captured by the existing flocs and (b) floc–floc aggregation occur, leading to a change in flocculation kinetics. This is reflected in a change in L_{eq} and k_b but especially in a growth in $L(0)$ as the "primary" particle is not a mineral clay particle anymore but a floc. For time intervals such that $\Delta t > 1500$ s, $L(t)$ is not a function of Δt anymore as $L(t > 1500\ s)$ has reached a constant value. In that case, it is found that the average value of $L(0)$ is about 60 μm, which can be considered as a good estimate for the primary floc size over the whole experimental range.

From this study, and the results illustrated in Fig. 5 (left), it can be concluded that the same fitting parameters cannot be used for the (fast) flocculation of unbonded mineral clay and polyelectrolyte strands or for the flocculation of already formed flocs. This is why it was proposed in Chassagne (2021) to separate SPM in two classes: one class (Class 1) being defined as unflocculated clay mineral particles and one class (Class 2) that is composed of flocs (mineral clay bound to organic matter). The mass transfer from Class 1 to Class 2 then obey the fast kinetics observed here at small Δt whereas the flocculation occurring in Class 2 (the aggregation of flocs lead to a new floc, that by definition belongs to Class 2) can be modelled, in good approximation, using the parameters found from fitting the data until an equilibrium size is reached ($\Delta t > 1500$ s).

In the following two sections, where the dependence on clay concentration and shear will be investigated, two time intervals will be studied: $\Delta t = 400$ s and $\Delta t = \Delta t_{end}$, whereby Δt_{end} represents the time interval between the start and the end of the experiment. In all cases the mean particle size $L(t)$ has reached a constant value when the time corresponding to the end of the experiment is reached.

4.2. Dependence on clay concentration

The dependence of $L(t)$ on clay concentration was studied for concentrations between 0.4 and $1.6\,g\,L^{-1}$ which is within the concentration range for which the measurements are not limited by light detection issues. A constant shear rate of $112\,s^{-1}$ is used in all experiments. The time evolution of the mean particle size is given in Fig. 6. Every experiment was replicated 3 or 4 times. The error bars in Fig. 6 (right) represent the standard deviation when averaging over all experiments. The parameters used for fitting the data shown in this figure are given in Table 1. As the parameter a_b was not changing much with clay concentration, the average value of a_b overall concentrations was chosen for each time series.

From the fit values for all clay concentrations used, the concentration dependence of L_{eq} and $k_b \simeq 1/t_b$ can be studied, see Figs. 7 and 8. Eq. (43) tells that at short Δt the flocculation rate should be linearly proportional to concentration. This is indeed found, even though the dependence on clay concentration is rather mild. For $\Delta t = \Delta t_{end}$ it is found that $t_b \simeq 1/k_b$ does not significantly depend on clay concentration. At short times, see Fig. 8, it is observed that the flocculation rate $(dL/dt)_{t\to 0}$ is increasing with clay concentration. It follows that $(dL/dt)_{t\to 0}$ scales with L_{eq} (not shown) since L_{eq} is increasing linearly

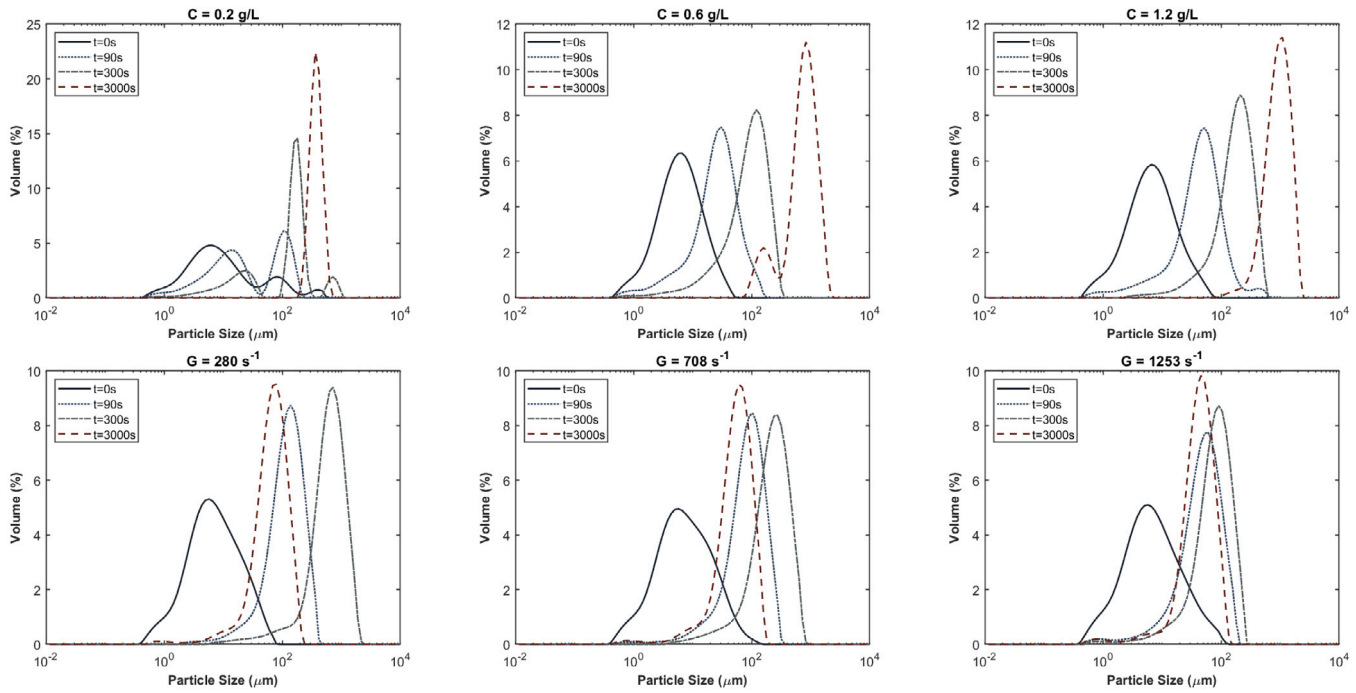

Fig. 3. Top panel: Particle size distributions for different clay concentrations (2.5 mg/g flocculant (Zetag 4110) to clay ratio). A constant shear rate of 112 s^{-1} is applied. Bottom panel: Particle size distributions for different shears (2.5 mg/g flocculant (Zetag 4110) to clay ratio, 1.2 g/L clay.

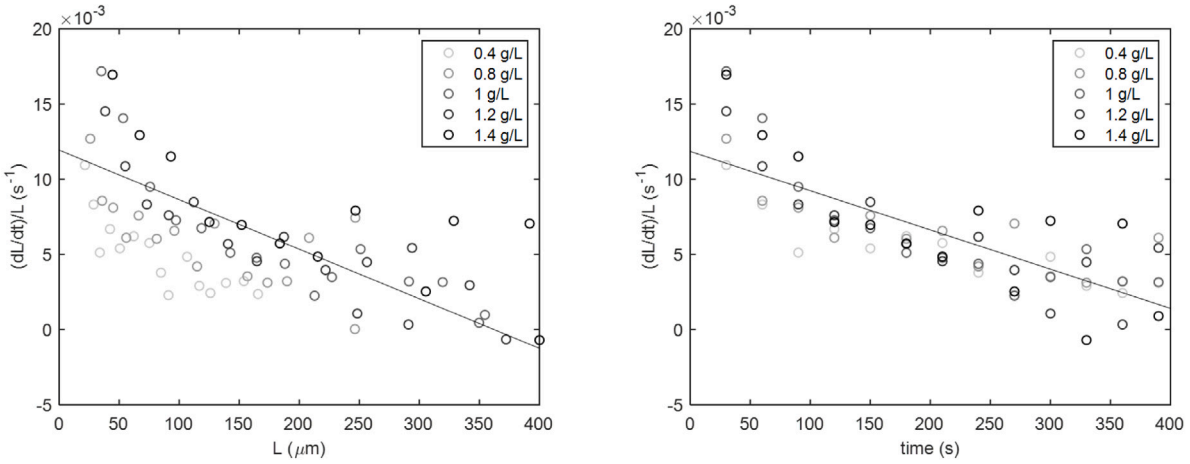

Fig. 4. (dL/dt)/L as function of L and time, for suspensions having 2.5 mg/g flocculant (Zetag 4110) to clay ratio. A constant shear rate of 112 s^{-1} is applied. The curves represent fits for 1.2 g/L.

Table 1
Fit parameters related to Fig. 6.

c (g/L)	$\Delta t = 400$ s				$\Delta t = \Delta t_{end}$			
	L_{eq} (μm)	t_b (s)	a_b	k_b (s^{-1})	L_{eq} (μm)	t_b (s)	a_b	k_b (s^{-1})
0.4	151	79	20	0.011	620	423	10.5	0.0021
0.6	145	98	20	0.009	598	368	10.5	0.0025
0.8	210	81	20	0.011	660	257	10.5	0.0035
1.0	269	81	20	0.011	928	277	10.5	0.0032
1.2	297	75	20	0.012	889	295	10.5	0.0030
1.4	469	85	20	0.011	918	202	10.5	0.0045
1.6	460	83	20	0.011	1013	208	10.5	0.0043

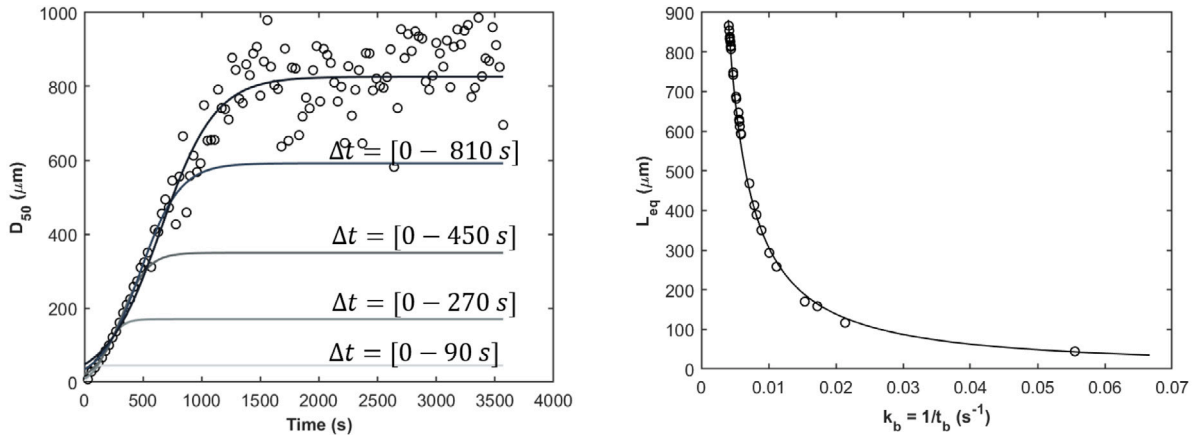

Fig. 5. Left: Particle size evolution as function of time, for a suspension consisting of 1.2 g/L clay and 2.5 mg/g flocculant (Zetag 4110) to clay ratio. A constant shear rate of 112 s^{-1} is applied. The curves represent fits for given time intervals as indicated next to each curve. The curve without indication represents the fit for the whole duration of the experiment. Right: L_{eq} as function of k_b found from fitting the particle size evolution as function of time for different time intervals Δt.

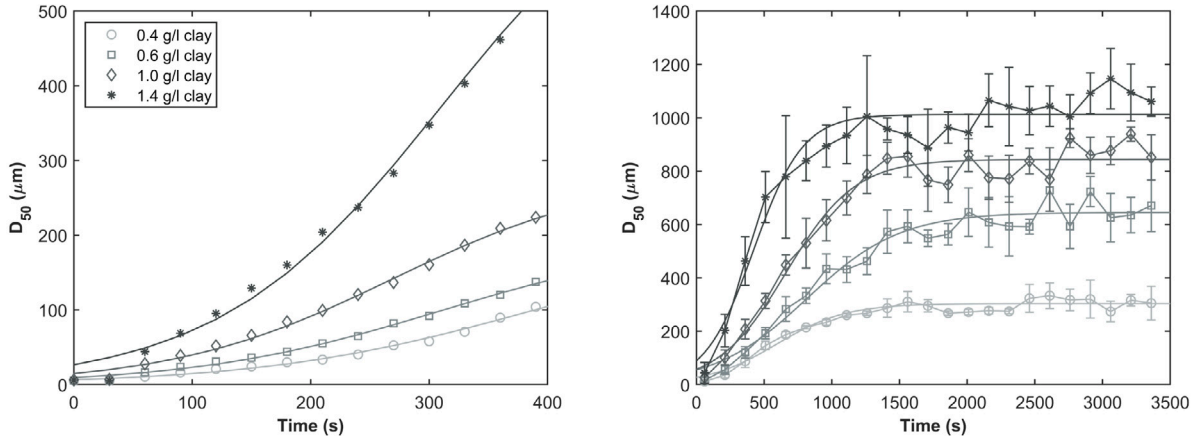

Fig. 6. Left: D_{50} as function of time for the onset of flocculation; Right: D_{50} as function of time for the whole duration of the experiments. The error bars indicate the differences observed when averaging over 3 or 4 measurements; the curves indicated the fits; the parameters for the fit are given in Table 1. The flocculant (Zetag 4110) to clay ratio is 2.5 mg/g.

with clay concentration, see Fig. 7. It was observed that the low shear rate of 112 s^{-1} did not produce a continuous flow of flocs in the pipes. Repeated measurements have confirmed that this shear rate leads to a large experimental error, as is clear from Fig. 6. For this reason, this shear rate was not used in subsequent shear rate dependence measurements, where only higher shear rates were used, which produced a continuous flow of flocs in the pipes. The advantage of working at 112 s^{-1} is that, in contrast to the shear experiments presented in the next section, the data can be fitted using only a birth function.

4.3. Dependence on shear

In order to study the effect of shear on the flocculation rate, experiments were performed at different shears, for a given clay concentration of 1.2 g L^{-1} and flocculant (Zetag 4110) to clay concentration ratio of 2.5 mg g^{-1}. Three examples of particle size distribution at different shear are given in Fig. 3(bottom panel). The time evolution of the mean particle size is given in Fig. 9. Every experiment was reproduced 3 or 4 times, leading to the error bars represented in the figure. The parameters used for fitting the data shown in this figure are given in Table 2. As the parameter a_b was not changing much with shear and time Δt, the average value of a_b overall shears was chosen for all-time series. At short times (Δt = 400 s) only a birth function was used for the fit.

As discussed in Shakeel et al. (2020), after a shearing period at sufficiently high shear, the dangling ends of flocs tend to coil, and the flocs get smaller until they reach a size that is in good approximation equal to the Kolmogorov microscale, see Fig. 9. In order to fit the decrease of L over time, it is necessary to introduce a decay term, as shown in Section 4.3. This decay is associated with a large characteristic time t_d resulting in a small k_d as in good approximation $t_d \simeq 1/k_d$. The associated parameters are given in Table 2. It was found that the parameter a_d was not changing much with shear, and it was therefore taken equal to its average value over all shears.

From the fit values for all shears used, the shear dependence of L_{eq} and k_b can be studied, see Figs. 7 and 8. The decrease of L_{eq} with shear is modelled by:

$$L_{eq}(\Delta t = 400s) = 5 \times 10^6 G^{-1.56}$$
$$L_{eq}\left(\Delta t = \Delta t_{end}\right) = 1 \times 10^6 G^{-1.52} \quad (46)$$

where it should be noted that L_{eq} is given in μm. For both Δt = 400 s and $\Delta t = \Delta t_{end}$ it is found that k_b is proportional to shear between 281

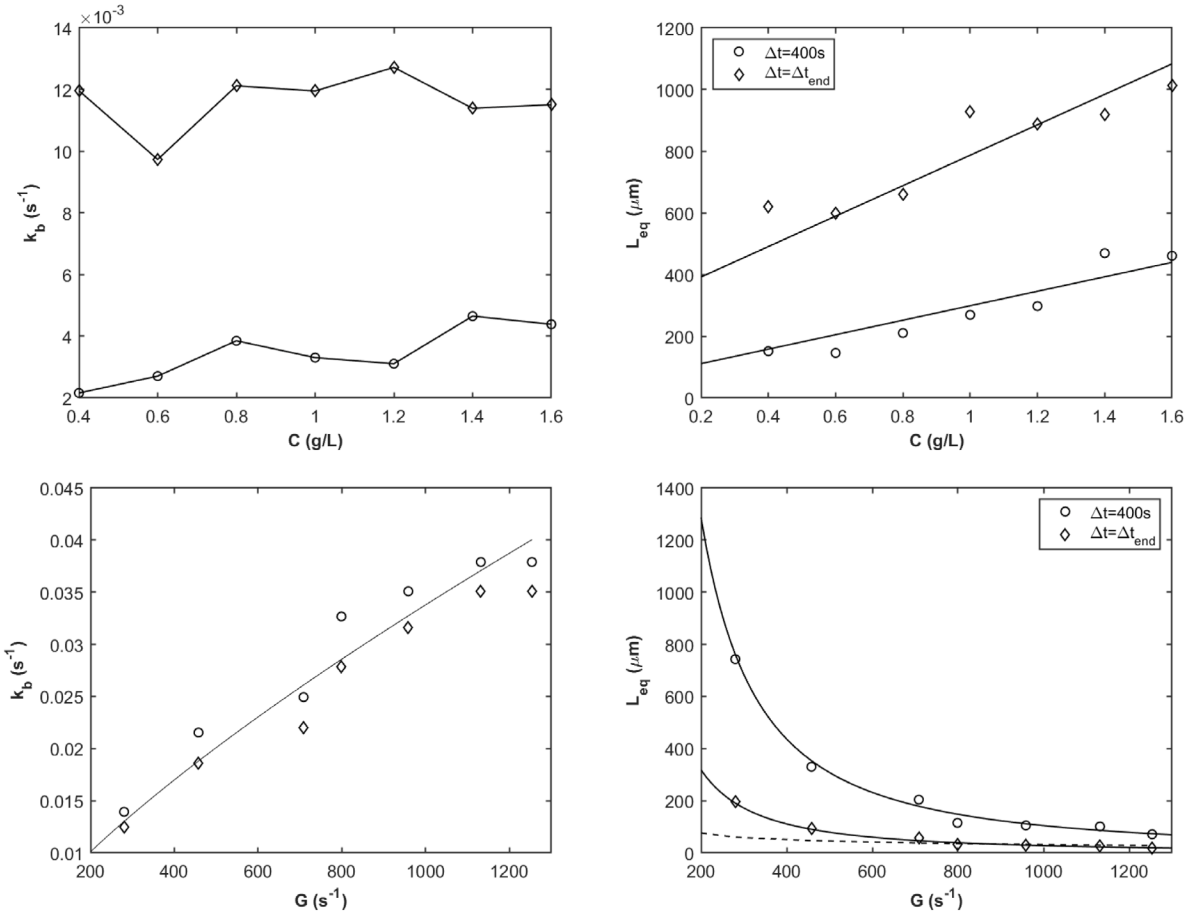

Fig. 7. k_b and L_{eq} as function of clay concentration c (g/L) and shear G (s^{-1}). All suspensions have 2.5 mg/g flocculant (Zetag 4110) to clay ratio. A constant shear rate of 112 s^{-1} is applied for the concentration dependence figures. A clay concentration of 1.2 g/L is used on the shear rate dependence figures. The curves represent fits as indicated in the text.

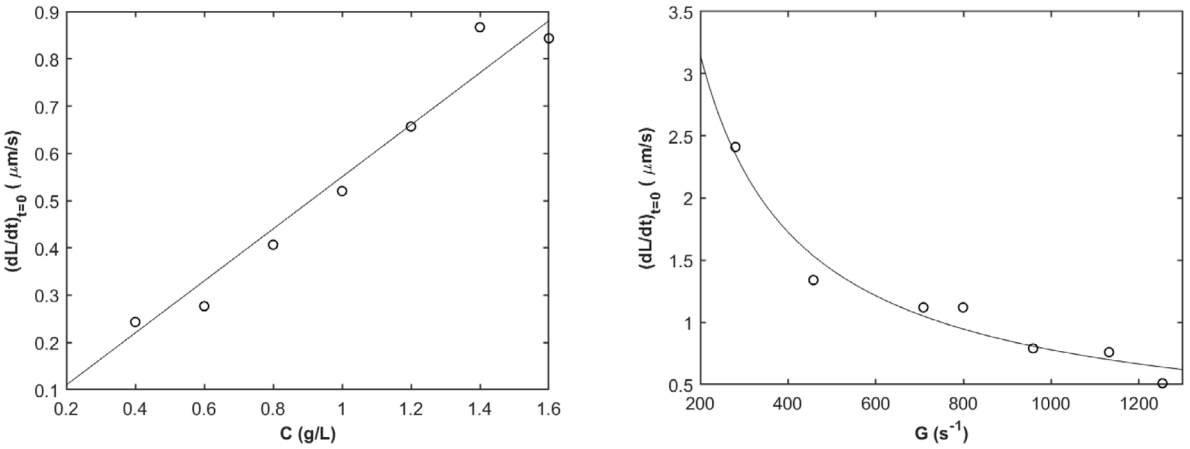

Fig. 8. The slope at origin $(dL/dt)_{t\geq 0}$ as function of clay concentration c (g/L) and shear G (s^{-1}). All suspensions have 2.5 mg/g flocculant (Zetag 4110) to clay ratio. A constant shear rate of 112 s^{-1} is applied for the concentration dependence figures. A clay concentration of 1.2 g/L is used on the shear rate dependence figures. The curves represent fits as indicated in the text.

s^{-1} and 1336 s^{-1} (see Table 2 and Fig. 7) according to:

$$k_b \simeq \frac{1}{t_b} \simeq 1.9 \times 10^{-4} G^{0.75} \tag{47}$$

This leads to the following correlation between L_{eq} and k_b:

$$\begin{aligned} L_{eq}\left(\Delta t = 400s\right) &\simeq 0.022 k_b^{-2.07} \\ L_{eq}\left(\Delta t = \Delta t_{end}\right) &\simeq 0.1 k_b^{-2.07} \end{aligned} \tag{48}$$

where again L_{eq} is given in μm. At high shear (> 700 s^{-1}) and $\Delta t = \Delta t_{end}$ it is found that L_{eq} follows the trend predicted by the Kolmogorov microscale, and therefore can be approximated by:

$$L_{eq}\left(\Delta t = \Delta t_{end}, G > 700\ s^{-1}\right) = \left(\frac{G}{\upsilon}\right)^{-0.5} \tag{49}$$

where $\upsilon = 10^{-6}$ m^2/s is the kinematic viscosity of water. As is clear from Fig. 7, for $G > 700$ s^{-1} the curves representing Eqs. (46),

Table 2
Fit parameters related to Fig. 9.

G (s^{-1})	$\Delta t = 400$ s				$\Delta t = \Delta t_{end}$						
	L_{eq} (μm)	t_b (s)	a_b	k_b (s^{-1})	L_{eq} (μm)	t_b (s)	a_b	k_b (s^{-1})	t_d (s)	a_d	k_d (s^{-1})
281	743	68	18	0.014	195	76	18	0.012	3382	3.5	2.3×10^{-4}
427	330	44	18	0.021	93	51	18	0.018	1319	3.5	5.9×10^{-4}
635	204	38	18	0.025	56	43	18	0.022	1246	3.5	6.2×10^{-4}
807	115	29	18	0.032	32	34	18	0.027	869	3.5	8.9×10^{-4}
958	105	27	18	0.035	28	30	18	0.031	931	3.5	8.3×10^{-4}
1147	101	25	18	0.038	26	27	18	0.035	1249	3.5	6.2×10^{-4}
1336	71	25	18	0.036	17	27	18	0.033	2198	3.5	3.5×10^{-4}

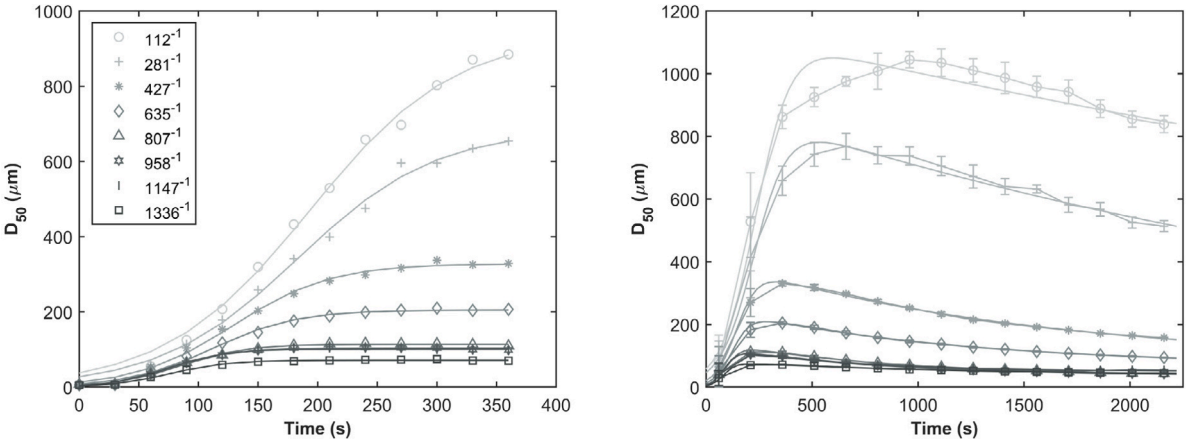

Fig. 9. Left: D_{50} as function of time for the onset of flocculation; the curves indicated the fits; Right: D_{50} as function of time for the whole duration of the experiments. The error bars indicate the differences observed when averaging over 3 or 4 measurements; the parameters for the fit are given in Table 2; The flocculant (Zetag 4110) to clay ratio is 2.5 mg/g for 1.2 g/L clay.

(49) are in close agreement and the difference in power of G is not noticeable. Eqs. (46) can therefore be used for the whole range of shear investigated.

The slope at origin $(dL/dt)_{t\to 0}$ decreases with G, which is in line with the estimation obtained from Eq. (48), using Eq. (8):

$$(dL/dt)_{t\to 0} = k_B L(t\to 0) \simeq k_b^{-1.07} \simeq G^{-0.8} \tag{50}$$

The fit (black curve in Fig. 8) gives, with $(dL/dt)_{t\to 0}$ in μm/s:

$$(dL/dt)_{t\to 0} = 313G^{-0.8} \tag{51}$$

5. Conclusions

In this article, two models for flocculation, one based on logistic growth theory (LG model) and the other on Smoluchowski's approach (S model), have been compared. Two series of experiments have been used for the comparison to explore the dependence of the model parameters on shear and clay concentration. It was found that kinetics of flocculation can be modelled with the LG model, whereas the S model does not reproduce the observed dependence on time of the mean floc size (D_{50}) represented by $L(t)$. By fitting the time evolution of $L(t)$, it was found that both the equilibrium floc size L_{eq} and t_b which are parameters for the LG model are a function of the time interval used for fitting. This was linked to the change in flocculation kinetics over time: at the onset of the experiment, the flocculation is dominated by the aggregation of unbonded mineral clay to polyelectrolyte strands, whereas at larger times, the flocculation is dominated by floc–floc aggregation. It was found that the floc–floc aggregation could be modelled over the whole experimental time interval with the same parameters, using the LG model. As has already been reported (Elimelech et al., 1995; Shakeel et al., 2020), flocs created by the addition of polyelectrolyte re-conform in the flow over time. This leads to a decrease in floc size at long time scales. The LG model can be used to model both growth and decay occurring over time, from which the characteristic timescales for growth and decay can be found. Not accounting for this decrease occurring at a long time, a general fitting function for a system of suspended clay destabilized by the addition of flocculant is found using Eqs. (46), (47) and is given by:

$$L(t) = a_L c G^{-1.5} \frac{1}{1 + a_b exp\left(-a_t G^{0.75} t\right)} \tag{52}$$

where a_L, a_b and a_t are empirical parameters that do not depend on concentration nor shear. These parameters, however, are expected to be function of the flocculant to clay ratio, which in the present study was kept constant. To give an order of magnitude, based on the fits reported in the current article, $a_L \simeq 5\times10^6$ (μm L g^{-1} $s^{1.5}$), $a_b \simeq 20$ and $a_t \simeq 2\times10^{-4}$ ($s^{-0.25}$). Eq. (52) can be differentiated to:

$$\frac{dL}{dt} = a_b a_t G^{0.75} \frac{exp\left(-a_t G^{0.75} t\right)}{1 + a_b exp\left(-a_t G^{0.75} t\right)} L \tag{53}$$

Eq. (53) is of the type that can be implemented in a sediment transport model.

Declaration of competing interest

The authors declare that they have no known competing financial interests or personal relationships that could have appeared to influence the work reported in this paper.

Acknowledgements

This work is performed in the framework of PlumeFloc (TMW.BL.019.004, Topsector Water and Maritiem: Blauwe route) within the MUDNET consortium. The authors would like to thank Deltares for using their experimental facilities in the framework of the MoU between TU Delft/Deltares.

Appendix

In this appendix, the derivations given in Winterwerp (1998) are discussed.

A.1. Aggregation term

Combining Eqs. (21) and (22) leads to

$$\frac{dn}{dt} = -\frac{8}{3}\alpha G L_i^3 n^2 \tag{54}$$

This equation is to be compared with Eq. (11) used by Winterwerp (1998) which reads

$$\frac{dn}{dt} = -\frac{3}{2}\pi e_c e_d G L^3 n^2 \tag{55}$$

The parameter e_c is defined by Winterwerp as "the efficiency parameter is a function of the physicochemical properties of the sediment and water and of the organic compounds in the sediment". The efficiency parameter e_d is defined by Winterwerp as "an (efficiency) parameter for diffusion". The product $e_c e_d$ can therefore be seen as the collision efficiency

$$\alpha = e_c e_d \tag{56}$$

The origin of the $\frac{3}{2}\pi$ in Eq. (55) is unknown. Combining Eqs. (17) and (18) yields

$$\phi_{\text{pp in floc}} = \frac{\rho_{floc} - \rho_w}{\rho_s - \rho_w} = \frac{c/\rho_s}{nV} \tag{57}$$

which is to be compared with Eq. (2) of Winterwerp (1998), which reads

$$\phi = \frac{\rho_s - \rho_w}{\rho_{floc} - \rho_w}\frac{c}{\rho_s} = f_s n L^3 \tag{58}$$

where Winterwerp uses $V = f_s L^3$, the shape factor f_s being equal to $\pi/6$ for spherical flocs. Note that the ϕ defined by Winterwerp corresponds to

$$\phi = \frac{\phi_s}{\phi_{\text{pp in floc}}} \tag{59}$$

and not to ϕ_s as he claims. Combining Eqs. (20), (22) and (23), gives

$$\frac{dL}{dt} = \frac{2\alpha G}{D}\frac{c}{\rho_s}\frac{L^{4-D}}{L_p^{3-D}} = k_A c G L^{4-D} \tag{60}$$

which corresponds with Eqs. (14,15) proposed by Winterwerp but for a different prefactor originating from the difference between Eqs. (54), (55).

A.2. Break-up term

The simplest models assume that s, defined in Eq. (26), scales with the size of particles, i.e. $p = 1$. However, in the case of fractal flocs as the ones formed by salt-induced aggregation of hard spheres, the smaller the fractal dimension, the less particle bonds per aggregate volume, the smaller the floc strength. Therefore the breakage rate should increase with decreasing fractal dimension D, which Barthelmes (Barthelmes et al., 2003) accounts for by introducing the term:

$$V_p^{1/3}\left(\frac{L}{L_p}\right)^{3/D} \tag{61}$$

in Eq. (26) to yield:

$$s = s_b\left(\frac{\eta G}{\tau^*}\right)^q V_p^{1/3}\left(\frac{L}{L_p}\right)^{3/D} \tag{62}$$

Note that this implies that:

$$p = 3/D \tag{63}$$

The break-up rate given by Winterwerp by (see Eqs. (16,17) in Winterwerp, 1998) is:

$$s = \frac{a}{T}\left(\frac{\eta G}{\tau^*}\right)^{q^*}\left(\frac{L - L_p}{L_p}\right)^{p^*} \tag{64}$$

where we substituted the turbulence induced stress $\tau_t = \eta G$ (Eq. (21) in Winterwerp, 1998). In our notation $\tau_y = \tau^*$ is the strength of floc. The parameters a, p^* and q^* are empirical. The parameter T is defined by Winterwerp as "the time scale of the disrupting eddies" which he assumes to be $T \simeq 1/G$.

Winterwerp furthermore follows the reasoning of Kranenburg (Kranenburg, 1994) which estimates that:

$$\tau^* \simeq n_b F \tag{65}$$

where F is the rupture force of a bond (N) which is implicitly assumed not to depend on L and n_b is the number of bonds per unit area. Because of the self-similarity property of fractals, it follows that $n_b = m_0/L^2$ where m_0 is a constant, and hence:

$$\tau^* \simeq \frac{m_0}{L^2}F \tag{66}$$

The fact that τ^* then scales with L^{-2} is therefore purely a consequence of assuming flocs to be fractal objects. The relation between floc's rupture and size has been experimentally tested whereby a single floc is pulled apart in tensile mode (Yeung and Pelton, 1996). It has been demonstrated that the rupture depends on the fractal dimension of the floc: it is the narrowest section cross-section in a fractal object which determines its strength, which does not need to be correlated with particle size. For compact flocs (high fractal dimension), the weak points are on the periphery, and therefore these flocs are prone to experience surface erosion. For low fractal dimension flocs, on the other hand, their narrowest cross-sections can be located anywhere, and hence they tend to break in two. This latter case is in line with the initial assumption that all flocs are assumed to have the same size at all times. It follows that Eq. (64) can be written:

$$s = aG\left(\frac{\eta G}{F}L^2\right)^{q^*}\left(\frac{L - L_p}{L_p}\right)^{p^*} \tag{67}$$

For situations where $L \gg L_p$ one gets:

$$s = \frac{aG^{q^*+1}}{L_p^p}\left(\frac{\eta}{F}\right)^{q^*} L_p^{2q^*+p^*} \tag{68}$$

Comparing Eqs. (62), (68), one finds the equivalence

$$\begin{aligned} q &= q^* + 1 \\ p &= 2q^* + p^* \end{aligned} \tag{69}$$

Winterwerp uses $p^* = 1$ and $q^* = 0.5$ which implies that $p = 2$ and $q = 1.5$. The fragmentation exponent q is usually found to be $1.5 < q < 6.5$ (Barthelmes et al., 2003) and as discussed above one usually assumes $3 \geq p \geq 1$.

From Eq. (15) one gets:

$$\frac{1}{n}\frac{dn}{dt} = -\frac{D}{L}\frac{dL}{dt} = e_b \times s \tag{70}$$

which leads to:

$$\frac{dL}{dt} = -e_b \times aG\left(\frac{\eta G}{F}L^2\right)^{q^*}\left(\frac{L - L_p}{L_p}\right)^{p^*} \times \frac{L}{D} \tag{71}$$

$$= -k_B G^{q^*+1}\left(L - L_p\right)^{p^*} L^{2q^*+1} \tag{72}$$

which is to be compared with Eqs.(22, 23) of Winterwerp (1998).

References

Barthelmes, G., Pratsinis, S.E., Buggisch, H., 2003. Particle size distributions and viscosity of suspensions undergoing shear-induced coagulation and fragmentation. Chem. Eng. Sci. 58 (13), 2893–2902.

Bouyer, D., Coufort, C., Line, A., Do-Quang, Z., 2005. Experimental analysis of floc size distributions in a 1-L jar under different hydrodynamics and physicochemical conditions. J. Colloid Interface Sci. 292 (2), 413–428.
Chassagne, C., 2020. Introduction to Colloid Science, Delft. Academic Press, ISBN: 9789065624376.
Chassagne, C., 2021. A simple model to study the flocculation of suspensions over time. Chem. Eng. Res. Des. 172, 302–311.
Chassagne, C., Safar, Z., 2020. Modelling flocculation: Towards an integration in large-scale sediment transport models. Mar. Geol. 430, 106361.
Deng, Z., He, Q., Safar, Z., Chassagne, C., 2019. The role of algae in fine sediment flocculation: in-situ and laboratory measurements. Mar. Geol. 71–84, 413.
Dyer, K.R., Manning, A.J., 1999. Observation of the size settling velocity and effective density of flocs, and their fractal dimensions. J. Sea Res. 41 (1–2), 87–95.
Elimelech, M., Gregory, J., Jia, X., Williams, R., 1995. Particle Deposition and Aggregation: Measurement, Modelling and Simulation. Butterworth-Heinemann.
Fettweis, M., 2008. Uncertainty of excess density and settling velocity of mud flocs derived from in situ measurements. Estuar. Coast. Shelf Sci. 78 (2), 426–436.
Flesch, J.C., Spicer, P.T., Pratsinis, S.E., 1999. Laminar and turbulent shear-induced flocculation of fractal aggregates. AIChE J. 45 (5), 1114–1124.
Gratiot, N., Manning, A.J., 2004. An experimental investigation of floc characteristics in a diffusive turbulent flow. J. Coastal Res. SI (41), 105–113.
Ibanez Sanz, M., 2018. Flocculation and Consolidation of Cohesive Sediments under the Influence of Coagulant and Flocculant (Ph.D. thesis). Technical University of Delft, Netherlands.
Khelifa, A., Hill, P.S., 2006. Models for effective density and settling velocity of flocs. J. Hydraul. Res. 44 (3), 390–401.
Kranenburg, C., 1994. The fractal structure of cohesive sediment aggregates Estuarine. Coastal Shelf Sci. 39 (6), 451–460.
Kusters, K., 1991. The Influence of Turbulence on Aggregation of Small Particles in Agitated Vessels (Ph.D. thesis). Eindhoven University of Technology, Eindhoven, The Netherlands.
Langmuir, I., 1918. The adsorption of gases on plane surface of glass mica and platinum. J. Am. Chem. Soc. 40 (9), 1361–1402. http://dx.doi.org/10.1021/ja02242a004.
Lesser, G., R, Roelvink, J., V, Van Kester, J., Stelling, G., 2004. Development and validation of a three-dimensional morphological model. Coastal Eng. 51 (8-9), 883–915.
Maggi, F., 2013. The settling velocity of mineral biomineral, and biological particles and aggregates in water. J. Geophys. Res. Oceans 118 (4), 2118–2132.
Manning, A.J., Bass, S.J., Dyer, K.R. and, 2006a. Floc properties in the turbidity maximum of a mesotidal estuary during neap and spring tidal conditions. Mar. Geol. 235 (1-4), 193–211.
Manning, A.J., Dyer, K.R., 2002. A comparison of floc properties observed during neap and spring tidal conditions. Proc. InMar. Sci. 5, 233–250.
Manning, A.J., Dyer, K.R., 2007. Mass settling flux of fine sediments in northern European estuaries: measurements and predictions. Mar. Geol. 245 (1–4), 107–122.
Manning, A.J., Whitehouse, R., Uncles, R. and, 2006b. Suspended particulate matter: the measurements of flocs. pp. 211–260.
Many, G., Bourrin, F., de Madron, X.D., Pairaud, I., Gangloff Verney, R., Menniti, C., Le Berre, D., 2016. Particle assemblage characterization in the rhone river rofi. J. Mar. Syst. 157, 39–51.
Mehta, A.J., 2014. an Introduction to Hydraulics of Fine Sediment Transport. World Scientific, Hackensack, N. J.
Normant, C.L., 2000. Three-dimensional modelling of cohesive sediment transport in the loire estuary. Hydrol. Process. 14 (13), 2231–2243.
Russel, W.B., Saville, D.A., Schowalter, W.R., 1989. Colloidal Dispersions. Cambridge University Press.
Safar, Z., Rijnsburger, S., Sanz, M.I., Chassagne, C., Manning, A., Pietrzak, J., Souza, A., Kessel, T.van., Horner-Devine, A., Flores, R., McKeon, M., 2019. Characterization and dynamics of suspended particulate matter in the near field of the rhine river plume during a neap tide. In: Geophysical Research Abstracts (Vol. 21).
Shakeel, A., Safar, Z., Ibanez, M., Paassen, L., Chassagne, C., 2020. Flocculation of clay suspensions by anionic and cationic polyelectrolytesa systematic analysis. Minerals 1–24.
Shen, X., Lee, B.J., Fettweis, M., Toorman, E.A., 2018. A tri-modal flocculation model coupled with TELEMAC for estuarine muds both in the laboratory and in the field. Water Res. 145, 473–486.
Soulsby, R.L., Manning, A.J., Spearman, J., Whitehouse, R.J.S., 2013. Settling velocity and mass settling flux of flocculated estuarine sediments. Mar. Geol. 339, 1–12.
Spearman, J.R., Manning, A.J., Whitehouse, R.J.S., 2011. The settling dynamics of flocculating mud:sand mixtures: Part 2 - numerical modelling. Ocean Dyn. http://dx.doi.org/10.1007/s10236-011-0385-8.
Spencer, K.L., Manning, A.J., Droppo, I.G., Leppard, G.G., Benson, T., 2010. Dynamic interactions between cohesive sediment tracers and natural mud. J. Soils Sedim. 10 (7), http://dx.doi.org/10.1007/s11368-010-0291-6.
Spicer, P., Pratsinis, S., 1996. Coagulation and fragmentation: Universal steady-state particle-size distribution. AIChE J. 42 (6), 1612–1620.
Van Leussen, W., 1988. Aggregation of Particles Settling Velocity of Mud Flocs A Review in Physical Processes in Estuaries. Springer, Berlin, Heidelberg, pp. 347–403.
Verney, R., Lafite, R., Brun-Cottan, J.C., Hir, P.Le., 2011. Behaviour of a floc population during a tidal cycle: laboratory experiments and numerical modelling. Cont. Shelf Res. 31 (10), S64–S83.
Winterwerp, J.C., 1998. A simple model for turbulence induced flocculation of cohesive sediment. J. Hydraul. Res. 36 (3), 309–326.
Yeung, A., Pelton, R., 1996. Micromechanics: a new approach to studying the strength and breakup of flocs. J. Colloid Interface Sci. 184 (2), 579–585.